Heliyon

CrossMark

New anthrarobin acyl derivatives as butyrylcholinesterase inhibitors: synthesis, *in vitro* and *in silico* studies

Mehreen Lateef [a], Abid Azhar [b], Bina S. Siddiqui [c], Shamshad Zarina [d], Nizam uddin [c],
Muhammad F. Anwar [d], Kauser Siddiqui [a], Kaniz F. Azhar [a], Lubna Iqbal [a],
Rashad Mehmood [e],*, Shagufta Perveen [f]

[a] *Pakistan Council of Scientific and Industrial Research Laboratories Complex, Karachi-75280, Pakistan*

[b] *The Karachi Institute of Biotechnology and Genetic Engineering, University of Karachi, Karachi-75270, Pakistan*

[c] *International Center for Chemical and Biological Sciences, H. E. J. Research Institute of Chemistry, University of Karachi, Karachi-75270, Pakistan*

[d] *National Center for Proteomics, University of Karachi, Karachi-75270, Pakistan*

[e] *Department of Chemistry, University of Education, Vehari Campus, Vehari-61100, Pakistan*

[f] *Department of Pharmacognocy, College of Pharmacy, King Saud University, PO Box 2457, Riyadh11451, Saudi Arabia*

* Corresponding author.

E-mail address: rashadhej@gmail.com (R. Mehmood).

Abstract

To treat Alzheimer's disease (AD), the available candidates are effective only against mild AD or have side effects. So, a study was planned to synthesis new candidates that may have good potential to treat AD. A series of new anthrarobin acyl derivatives (**2–8**) were synthesized by the reaction of anthrarobin (**1**) and acetic anhydride/acyl chlorides. The product were characterized by ^{1}H NMR and EI-MS, and evaluated for butyrylcholinesterase (BuChE) inhibition activity. Compounds **5** and **4** showed notable BuChE inhibitory potential with IC_{50} 5.3 ± 1.23 and 17.2 ± 0.47 μM, respectively when compared with the standard eserine (IC_{50} 7.8 ± 0.27 μM), compound **5** showed potent BuChE inhibition potential than

the standard eserine. The active compounds **5** and **4** have acyl groups at 2-OH and 10-OH positions which may be responsible for inhibitory potential as this orientation is absent in other products. *In silico* studies of **5** and **4** products revealed the high inhibitory potential due to stable binding of ligand with the BuChE active sites with docking energy score −18.8779 kcal/mol and −23.1159 kcal/mol, respectively. Subsequently, compound **5** that have potent BuChE inhibitory activity could be the potential candidate for drug development for Alzheimer's disease.

1. Introduction

Alzheimer's disease (AD) is a chronic and progressive neurodegenerative disorder, characterized by memory impairment, cognitive dysfunction, and behavioral disturbances along with central cholinergic function loss (Aisen and Davis, 1997). AD has been found to be associated with cholinergic deficit and is characterized by significant decrease in acetylcholine (ACh) amount (Bachman et al., 1992). ACh is a neurotransmitter, its neurotransmitter action diminish by cleaving (Quinn, 1987) or inhibiting mainly by acetylcholinesterase (AChE) and BuChE, considered to be important in the pathology of AD (Hebert et al., 1995). Both enzymes present in the brain, as AChE is mostly located in neurons and BuChE is largely associated with glial cell (Wright et al., 1993). Normally, in the healthy brain, AChE accounts for 80% while BuChE accounts for remaining 20% role in regulating the brain cholinesterase (ChE) activity and also evidently play a role in AD pathology and disease progression. However, in AD patient's brain, AChE activity may be reduced to 55–67% while BuChE activity increases and BuChE is accumulated in neurons, glial cells, neurotic plaques and tangles (Greig et al., 2001; Perry et al., 1978). The most effective accepted treatment strategy against AD is the elevation of ACh amount through AChE enzyme inhibition (Arnold and Kumar, 1993). Therefore, AChE and BuChE inhibitors have become notable in the treatment of AD. However, the several present AChE inhibitors (rivastigmine, donepezil and tacrine) use for the treatment of AD possess some side effects, and secondly, effective only against mild type of AD and no BuChE inhibitors available to present (Schneider, 2001). A few BuChE inhibitors have been discovered, but still need to develop new drugs to treat AD effectively.

The ChE inhibitors specifically act on the enzymes that hydrolyze the ACh during synaptic release. The use of agents with enhanced selectivity for BuChE including cymserine and MF-8622 indicate potential therapeutic benefit of inhibiting BuChE in AD and related dementias. BuChE specific inhibition is unlikely to be associated with adverse events and may show efficacy without remarkable side effects (Greig et al., 2005; Woo et al., 2011). Therefore, BuChE may be considered as an

important target for novel drug development to treat AD. Henceforth, the development of specific BuChE inhibitors and continues use of ChE inhibitors may lead to improved clinical outcomes (Greig et al., 2005).

This paper describes the synthesis and BuChE inhibitory activity of novel anthrarobin acyl derivatives (**3–5**, **7–8**) while compounds **2** and **6** have been reported for their antioxidant potential by the same group (Lateef et al., 2015). Anthrarobin is a substituted polycyclic hydrocarbon and its derivatives have shown diverse activity depending on the nature of attach functional groups. Naturally isolated and synthetic anthrarobin derivatives are found to be active against 5-alpha (α) reductase, which is involved in production of benign prostatic hyperplastic and prostatic cancer (Woo et al., 2011). Anthrarobin (anthracene-1,2,10-triol) is also found to have xanthine oxidase inhibitory activity at 68.35 µM concentration (Sheu and Chiang, 1997). Any minute change in the existing structure of anthrarobin may reveal different biological activities and various pharmacological effects (Giacobini 2001; Hiipakka et al., 2002). Due to the potent and diverse activities of anthrarobin derivatives, this study was planned to synthesize and determine the BuChE inhibition activity of new anthrarobin derivatives. Furthermore, docking studies were also performed to understand interactions between ligand showing potent inhibitory activity and receptor.

2. Experimental

2.1. Material and methods

All the chemicals and solvents were purchase from Sigma and used as such. Thin layer chromatography (TLC) was performed on precoated 0.5 mm thick silica gel 60 F_{254} aluminum sheets. TLC plates were sprayed with 5% (v/v) aqueous solution of H_2SO_4, containing 4% (w/v) phosphomolybdic acid, 0.5% (w/v) ceric ammonium sulfate, and heated at 120 °C to visualize the spots. IR spectra were recorded on Shimadzu FTIR-8900 spectrometer (Shimadzu, Kyoto, Japan) as KBr pellets. ^1H NMR spectra were recorded on a Bruker AM-400 instrument (Bruker, Faellanden, Switzerland) in $CDCl_3$ solvent with tetramethylsilane as an internal standard. The chemical shifts are reported in ppm (δ) and coupling constant (J) are given in Hz. Mass spectra were obtained in an electron impact mode on Finnigan MAT-112 and MAT-113 spectrometers and ions are given in m/z (%).

2.2. General synthetic procedure of anthrarobin acyl derivatives (2–8)

An acetic anhydride or acyl chloride (1–3 ml) was added to a pyridine (2 ml) solution of anthrarobin (**1**; 100 mg, for each reaction), and the reaction mixture shortly warmed and left for overnight at room temperature. The mixture was then poured over crushed ice and extracted with ethyl acetate (AcOEt). The AcOEt

layer was washed with water, dried over anhydrous Na_2SO_4 and evaporated under reduced pressure to the product residue. The purity of the products was checked through TLC.

2.2.1. 1,10-Dihydroxyanthracene-2-acetate (2)

White powder; Yield: 23%; IR (KBr) ν_{max} cm^{-1}:3490 (OH), 1765 (ester), 1602–1415 (aromatic moieties), 1310 (O-C); ^{1}H NMR (CDCl$_3$, 400 MHz): δ = 12.7 (br. s, OH), 8.28–8.31 (3H, m, H-5, −7, −9), 7.85 (1H, d, J = 8.7 Hz, H-4), 7.78–7.82 (2H, m, H-6, −8), 7.45 (1H, d, J = 8.7 Hz, H-3), 2.39 (3H, s, CH$_3$CO); EIMS m/z: 268.0 [M]$^+$ C$_{16}$H$_{12}$O$_4$ (calcd. 268.0736).

2.2.2. 1,10-Dihydroxyanthracene-2-butanoate (3)

White powder; Yield: 29%; IR (KBr) ν_{max} cm^{-1}: 3505 (OH), 1768 (ester), 1610–1420 (aromatic moieties), 1304 (O-C); ^{1}H NMR (CDCl$_3$, 400 MHz): δ = 12.7 (br. s, OH), 8.29–8.31 (3H, m, H-5, −7, −9), 7.85 (1H, d, J = 8.4 Hz, H-4), 7.79–7.82 (2H, m, H-6, −8), 7.43 (1H, d, J = 8.4 Hz, H-3), 2.32 (2H, t, J = 7.6 Hz, CH$_2$CO), 1.61 (2H, m, CH$_2$CH$_2$CO), 0.89 (3H, t, J = 7.2 Hz, CH$_3$CH$_2$); EIMS m/z: 296.1 [M]$^+$ C$_{18}$H$_{16}$O$_4$ (calcd. 296.1049).

2.2.3. 1-Hydroxyanthracene-2,10-dibutanoate (4)

Yellow powder; Yield: 19%; IR (KBr) ν_{max} cm^{-1}: 3505 (OH), 1769 (ester), 1601–1400 (aromatic moieties), 1290 (O-C); ^{1}H NMR (CDCl$_3$, 400 MHz): δ = 12.7 (br. s, OH), 8.30 (1H, s, H-9), 8.28 (1H, d, J = 8.4 Hz, H-4), 8.25(1H, dd, J = 6.0, 3.2 Hz, H-5), 8.19 (1H, dd, J = 5.4, 3.2 Hz, H-7), 7.75–7.77 (2H, m, H-6, −8), 7.59 (1H, d, J = 8.4 Hz, H-3), 2.74 (2H, t, J = 7.4 Hz, CH$_2$CO(10)), 2.58 (2H, t, J = 7.6 Hz, CH$_2$CO(2)), 1.74–1.91 (4H, m, 2(CH$_2$CH$_2$CO)), 1.03–1.12 (6H, m, 2 (CH$_3$CH$_2$); C$_{22}$H$_{22}$O$_5$; EIMS m/z: 366.1 [M]$^+$ C$_{22}$H$_{22}$O$_5$ (calcd. 366.1467).

2.2.4. 1-Hydroxyanthracene-2,10-dihexanoate (5)

Yellow powder; Yield: 38%; IR (KBr) ν_{max} cm^{-1}: 3504 (OH), 1765 (ester), 1610–1415 (aromatic moieties), 1302 (O-C); ^{1}H NMR (CDCl$_3$, 400 MHz): δ = 12.7 (br. s, OH), 8.27–8.33 (4H, m, H-4, −5, −7, −9), 7.92 (1H, dd, J = 5.4, 3.2 Hz, H-8), 7.85 (1H, m, H-6), 7.44 (1H, d, J = 8.0 Hz, H-3), 2.78 (2H, t, J = 7.6 Hz, CH$_2$CO(10)), 2.65 (2H, t, J = 7.6 Hz, CH$_2$CO(2)), 1.77–1.94 (4H, m, 2 (CH$_2$CH$_2$CO)), 1.31–1.35 (8H, br., 2((CH$_2$)$_2$CH$_3$)), 0.89 (6H, m, 2(CH$_3$CH$_2$)); EIMS m/z: 422.2 [M]$^+$ C$_{26}$H$_{30}$O$_5$ (calcd. 422.2093).

2.2.5. Anthracene-1,2,10-triacetate (6)

Brownish powder; Yield: IR (KBr) ν_{max} cm^{-1}: 33.7%; 1772 (ester), 1609–1420 (aromatic moieties), 1309 (O-C); ^{1}H NMR (CDCl$_3$, 400 MHz): δ = 8.32 (1H, s, H-9), 7.99 (1H, m, H-5), 7.89 (1H, m, H-7), 7.86 (1H, d, J = 9.2 Hz, H-4), 7.49–7.52 (2H, m, H-6, −8), 7.34 (1H, d, J = 9.2 Hz, H-3), 2.61(3H, s, CH$_3$CO(1)), 2.52 (3H, s, CH$_3$CO(10)), 2.35 (3H, s, CH$_3$CO(2)); EIMS *m/z*: 352.1C$_{20}$H$_{16}$O$_6$ [M]$^+$ (calcd. 352.0947).

2.2.6. Anthracene-1,2,10-trihexanoate (7)

Yellowish powder; Yield: 33.7%; IR (KBr) ν_{max} cm^{-1}: 1765 (ester), 1610–1415 (aromatic moieties), 1298 (O-C); ^{1}H NMR (CDCl$_3$, 400 MHz): δ = 8.31 (1H, dd, J = 6.0, 3.2 Hz, H-5), 8.29 (1H, s, H-9), 7.95–7.99 (1H, m, H-7), 7.86–7.89 (1H, m, H-6), 7.82 (1H, d, J = 9.6 Hz, H-4), 7.79 (1H, dd, J = 6.0, 3.2 Hz, H-8), 7.32 (1H, d, J = 9.6 Hz, H-3), 2.89 (2H, t, J = 7.6 Hz, CH$_2$CO(1)), 2.78 (2H, t, J = 7.6 Hz, CH$_2$CO(10)), 2.58 (2H, t, J = 7.6 Hz, CH$_2$CO(2)), 1.75–1.96 (6H, m, 3 (CH$_2$CH$_2$CO)), 1.31–1.35 (12H, br., 3((CH$_2$)$_2$CH$_3$)), 0.91 (9H, m, 3(CH$_3$CH$_2$)); EIMS *m/z*: 520.2C$_{32}$H$_{40}$O$_6$ [M]$^+$ (calcd. 520.2825).

2.2.7. Anthracene-1,2,10-trioctanoate (8)

Yellowish powder; Yield: 22.3%; IR (KBr) ν_{max} cm^{-1}: 1770 (ester), 1605–1415 (aromatic moieties), 1305 (O-C); ^{1}H NMR (CDCl$_3$, 400 MHz): δ = 8.31 (H, dd, J = 5.6, 3.2 Hz, H-5), 8.29 (1H, s, H-9), 7.96–7.99 (1H, m, H-7), 7.86–7.89 (1H, m, H-6), 7.80 (1H, d, J = 9.6 Hz, H-4), 7.79 (1H, dd, J = 5.6, 3.2 Hz, H-8), 7.32 (1H, d, J = 9.6 Hz, H-3), 2.89 (2H, t, J = 7.6 Hz, CH$_2$CO(1)), 2.78 (2H, t, J = 7.6 Hz, CH$_2$CO(10)), 2.58 (2H, t, J = 7.6 Hz, CH$_2$CO(2)), 1.75–1.96 (6H, m, 3 (CH$_2$CH$_2$CO)), 1.31–1.35 (24H, br., 3((CH$_2$)$_4$CH$_3$)), 0.91 (9H, m, 3(CH$_3$CH$_2$)); EIMS *m/z*: 604.4C$_{38}$H$_{52}$O$_6$ [M]$^+$ (calcd. 604.3764).

2.3. Anticholinesterase assay

Anticholinesterase inhibition activity was determined by Ellman's spectrophotometric method (Ellman et al., 1961) using acetylcholinesterase as substrate and 5,5′-dithio-bis(2-nitrobenzoic) acid (DTNB) as chromogen. Horse butyrylcholinesterase (EC 3.1.1.8) was purchased from Sigma (St. Luios, MO, USA) and prepared by dissolving in phosphate buffer (100 mM, pH 8.0). The BuChE concentration was adjusted to 0.2 U per well. 180 µL of sodium phosphate buffer (pH 8.0) and 10 µL buffered Ellman's Reagent (DTNB, 0.1 M NaHCO$_3$) was added in wells labeled as blank (substrate and enzyme), control and test. 10 µL of test compound solution (conc. varies 5–500 µM) was added in each well labeled as test. Then, 20 µL of BuChE solution was added in each well including enzyme, control and test. The contents were mixed and incubated for 15 min at 25 °C. The reaction was then

initiated by adding 10 µL of substrate solution butyrylcholinesterase iodide (10 mM) in each well except enzyme. The hydrolysis of acetylthiocholine or butyrylthiocholine was determined by the formation of yellow 5-thio-2-nitrobenzoate anion as a result of the reaction with DTNB with thiocholines, catalyzed by enzymes at a wavelength of 412 nm. Methanol was used as negative control. Inhibition percentage was calculated according to Michaelis–Menten model by using "EZ-Fit. The IC_{50} values were determined by monitoring the inhibition effects of various concentrations of under investigation compounds and calculated EZ-Fit, Enzyme Kinetics Program (Perrella Scientific In., Amhherset, USA).

2.4. *In silico* (docking) analysis

2.4.1. *Preparation of molecules*

After performing enzyme inhibition analysis, newly synthesized compounds were subjected to *in silico* (docking) studies. For docking studies, 3D structure of receptor BuChE (PDB ID: 1POI) was obtained from PDB (http://www.rcsb.org). All ligands and water molecules were deleted, followed by addition of polar hydrogen. Structure of standard eserine (physostigmine, M.F.: $C_{15}H_{21}N_3O_2$) was obtained from Pubchem (CID 5983) in sdf format that was subsequently converted into mol2 format by using Open Babel GUI (graphical user interface) software (O'Boyle et al., 2011). *In silico* preparation of anthrarobin derivatives (lead compounds) was accomplished by using Accelrys Discovery Studio Visulaizer V2.5 in sketch mode. Gasteiger atomic partial charges were calculated for receptor and all lead compounds and Dreiding-like force field was applied to prepare the final molecules.

2.4.2. *Selection of binding cavity*

The BuChE active site gorge comprises of 55 amino acids and is ~ 200 Å^3 (Çokuğraş, 2003). Earlier studies have highlighted many critical residues including D70, W82, G116, G117, A119, A199, S198, L286, V288, E325, Y332 and H438 (Çokuğraş, 2003). Among these, D70 and Y332 are present at peripheral anionic site (PAS) and are crucial for preliminary binding of substrate (Masson et al., 1999). At the bottom of the 20 Å deep gorge, a catalytic triad of S198, H438 and E325 is located. The substrate specificity for catalysis of larger acyl group is determined by L286 and V288 (Çokuğraş, 2003; Masson et al., 1999; Kovarik et al., 2003; Nicolet et al., 2003). Recent inhibition studies reported that tacrine derivatives can interact differentially with D70, W82, T120, F278, F329, Y332 and H438 (Campiani et al., 2005; Macdonald et al., 2012). Therefore, residues that had been found common in multiple publications were considered as most crucial residues. Structural and physiological details regarding the active site pocket were obtained for the determination of binding site. In order to cover all the possible interactions within the binding pocket, D70, V288 and H438 were selected.

2.4.3. Docking analysis

FlexX (Rarey et al., 1996) was employed for docking purpose in batch mode. Standard (eserine) and lead candidates were docked on BuChE active site gorge using default parameters. The software was allowed to search for an optimal conformation and binding mode of each compound within 10 Å (default) radius of search sphere.

3. Results and discussion

3.1. Chemistry

The anthrarobin acyl derivatives **2**–**8** (Fig. 1) were prepared by reaction of anthrarobin (**1**) and acetic anhydride or acyl chlorides as described in the Experimental Part.

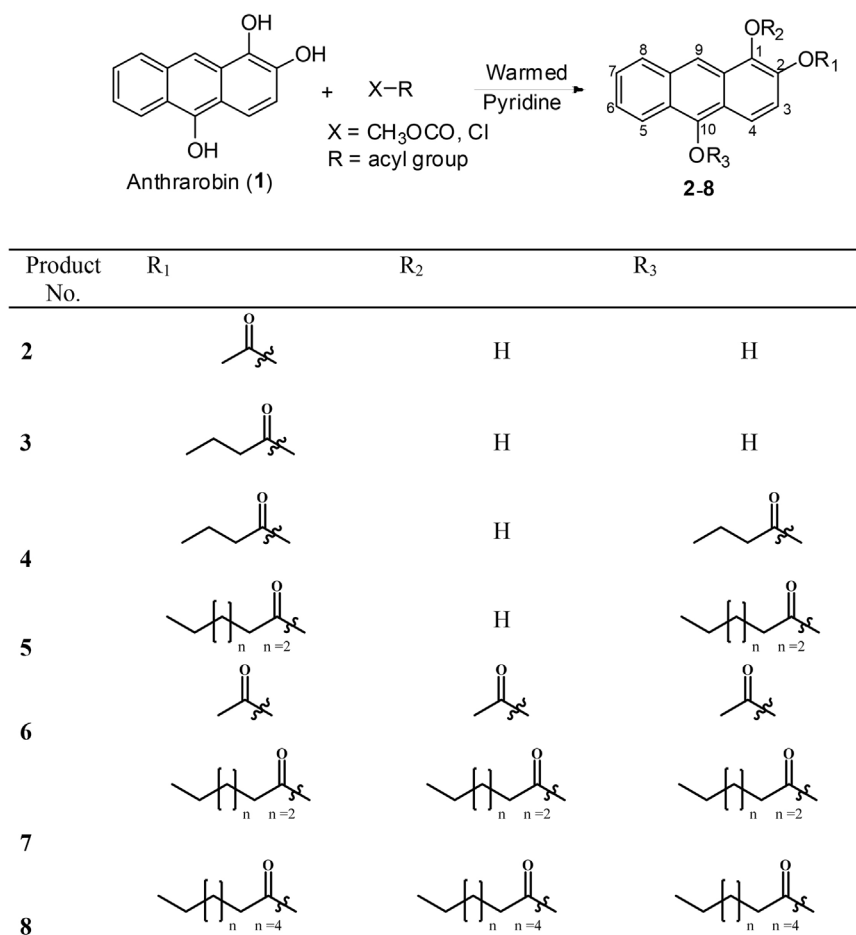| Product No.	R_1	R_2	R_3
2	(acetyl)	H	H
3	(acyl)	H	H
4	(acyl)	H	(acyl)
5	(acyl, $n=2$)	H	(acyl, $n=2$)
6	(acyl)	(acyl)	(acyl)
7	(acyl, $n=2$)	(acyl, $n=2$)	(acyl, $n=2$)
8	(acyl, $n=4$)	(acyl, $n=4$)	(acyl, $n=4$)

Fig. 1. Synthetic scheme of the products.

The IR spectra of the products showed the absorption bands in the ranges 1760–1772 and 1400–1610 cm^{-1} for the ester and aromatic moieties, respectively. The IR spectra of **2–5** also showed a broad absorption band in the range of 3470–3510 cm^{-1} for the free hydroxyl group. In the ^{1}H NMR spectra of the products (supplementary material), anthrarobin skeleton protons resonated in the range of δ 7.32–8.33. The carbonyl attached methyl protons exhibited singlets in the range of δ 2.25–2.38 and methylene protons exhibited triplet in the range of δ 2.32–2.36. The terminal methyl protons showed triplets in the range of δ 0.85–1.13. The first acyl groups were attached to the 2-OH because the lone pair of oxygen was less involved in the resonance. The second acyl groups whether attached with 1-OH or 10-OH, can be confirmed based on the downfield signals of the hydrogen bonded protons in the range of 11.7–12.7. The products **4** and **5** showed downfield signals at δ 11.7–12.5 confirming the second acyl group attached with the 10-OH. EI-MS spectral data also confirmed the number of acyl groups (mono, di or tri) in the products.

3.2. BuChE inhibition activity

All the products were screened for the BuChE inhibition activity. The products **4** and **5** showed outstanding BuChE inhibition activity while the other products showed non-significant activity (Table 1) when compared with the standard eserine. On the basis of structure-activity relationship, it is suggested that the position of the acyl groups may influence the BuChE inhibition activity. The active products have acyl groups at 2-OH and 10-OH position and this specific arrangement may favor to block the active sites of the BuChE enzyme.

Table 1. IC$_{50}$ values of butyryl cholinesterase inhibition activity of the products.

Compounds	Butyrylcholinesterase inhibition activity IC$_{50}$ μM $\pm$ SEM
Anthrarobin (**1**)	89.3 $\pm$ 0.21
1,10-Dihydroxyanthracene-2-acetate (**2**)	85.2 $\pm$ 0.21
1,10-Dihydroxyanthracene −2-butanoate (**3**)	>250
1-Hydroxyanthracene-2,10-dibutanoate (**4**)	17.2 $\pm$ 0.47
1-Hydroxyanthracene-2,10-dihexanoate (**5**)	5.3 $\pm$ 1.23
Anthracene-1,2,10-triacetate (**6**)	69.2 $\pm$ 0.40
Anthracene-1,2,10-trihexanoate (**7**)	Nil
Anthracene-1,2,10-trioctanoate (**8**)	>250
Eserine	7.8 $\pm$ 0.27

Values are expressed as mean of three experiments with standard error of the mean (SEM).

3.3. *In silico* studies

3.3.1. *In silico studies of Eserine*

For eserine, best pose gave an energy score of −15.6376 kcal/mol, in which 6 amino acids (W82, P285, A328, F329, Y332 and H438) showed interactions with ligand. Eserine formed one H-bonds with Pro285. H9 of eserine formed H-bond with O of proline side chain.W82 found to have 4H3C-π interactions 2 with each of C20 and C19 of eserine. H438 also have 2 H_3C-π interactions, one each with C20 and C19 of serine (Table 2). Ring 1 of eserine was found to form 4 π interactions: 1 each with A328, H438 and 2 with F329. Tyr332 showed three hydrophobic interactions with ring 1, C16 and N15-C14 bond pair of eserine. G116 was not directly interacting but seems to be the part of hydrophobic interacting loop (Fig. 2).

3.3.2. *In silico studies of 1-Hydroxyanthracene-2,10-dibutanoate (4)*

In the best pose, 11 amino acids of receptor (W82, G115, G116, G117, S198, A199, W231, A328, F329, Y332 and H438) (Table 2) interacted with ligand molecule with docking energy of − 23.1159 kcal/mol. O15 on aromatic ring system 2 of compound **4** formed 3H-bonds with α-amino groups of G116, G117 and A199 simultaneously, where the amino group of each amino acid acted as hydrogen bond donor. The hydroxyl group of S198 side chain, acted as an H-bond donor and acceptor for O26 of substituted group attached to C9 and O17 attached to C10 of ring 2, respectively. The sp^2 hybridized N and aromatic ring of H438 formed a H-bond with O17 (H-bond donor) and 4 horizontally displaced π- π interaction among which, two were with ring 1 and one each with ring 2 and ring 3 (Fig. 3).

The bond pairs of peptide bonds between G117-G116-G115 found to have 2 π interactions with ring 2 of **4**. There were five H_3C-π interactions observed between receptor and ligand, among which two were between W231 and C21, one in

Table 2. Scores of bonding pattern of three compounds.

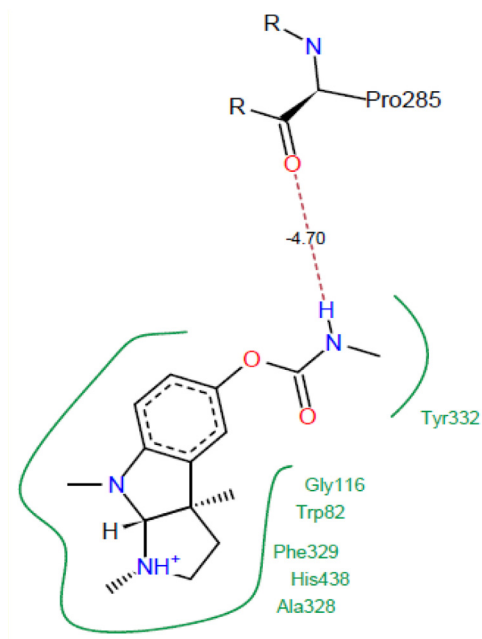| Eserine		1-Hydroxyanthracene-2,10-dibutanoate (4)	1-Hydroxyanthracene-2,10-dihexanoate (5)
W82	1 (~5 Å)	4 (~4.43 Å) + 1 (~4.32 Å)	5 (~3.84 Å)
G116	1 (~4 Å)		
G117			
F329	2 (at 5 Å)	3 (~4.1933 Å)	3 (~4.05 Å) + 1 (~4.97 Å)
H438	1 (4.2 Å) + 1 (3.75 Å) + 2 (4.5 Å)	2 (~4.13 Å)	2 (~4.08 Å)

Fig. 2. Eserine docked in BuChE binding pocket using FlexX software. Eserine forms H-bonds with P285 of the receptor. Stability as Energy minimization for interacting bond is depicted on bond representative line. Residues shown in green indicate hydrophobic interactions with ligand molecule.
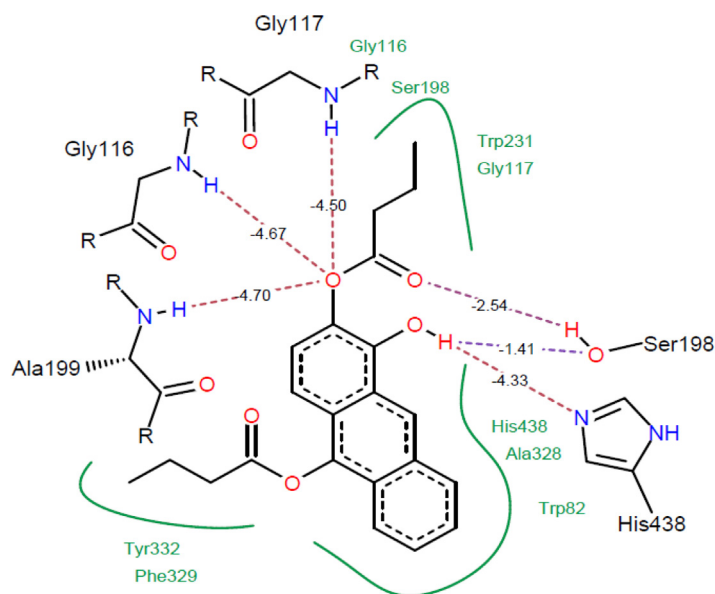

Fig. 3. 1-Hydroxyanthracene-2,10-dibutanoate (**4**) molecule docked in BuChE receptor. The docked conformation shows H-bonding of anthrarobin with G116, G117, S198, A199 and H438. Red lines represent strong interactions while blue lines show weak interaction. Stability as energy minimization (e.m.) for each bond is represented on the bond representative line. Residues shown in green indicate pi or hydrophobic interactions with ligand molecule.

between A328 and ring 3, one each between C25 and F329, C25 and Y332. The second tryptophan in the pocket, W82 formed 3 displaced π-π interactions with ring 3. Phenyl group of F329 was also found to make 4 horizontal π-π interactions, 2 interactions with each of between aromatic rings1 and 2 of ligand.

3.3.3. In silico studies of 1-Hydroxyanthracene-2,10-dihexanoate (5)

In the best pose, 9 amino acids (W82, G115, G116, G117, S198, A199, A328, F329, and H438) (Table 2) were shown to interact with ligand (-18.8779 kcal/mol energy score). Most of the interactions observed between compound **5** and receptor were similar to that of compound **4**, for instance A328, W82, G115-G116 bond pair, G116-G117 bond pair, F329 and H438 behaved with compound **5** similarly as with compound **4**, with the exception that the H438 accepts H-bond from O20 instead of O17 and having an additional T-stacking with ring 3 (Fig. 4).

Hydrogen bonds of G116, G117 and A199 were also retained with only exception that O19 of compound **5** was involved. Similarly, the interaction behavior of S198 was similar to that of compound **4** with an exception that the interacting atoms of ligand were O33 and O20. W82 also has two H_3C-π interactions with terminal C31 (terminal methyl) of substituted group attached C4 of Aromatic ring system 1. Here
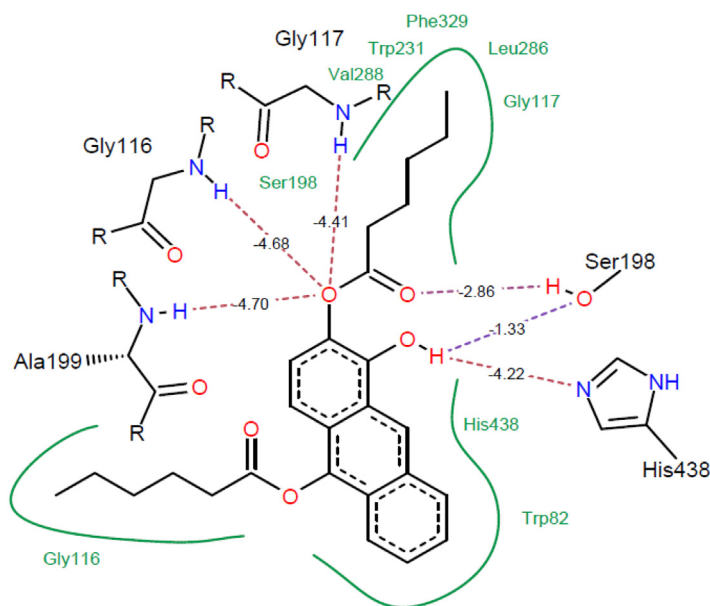

Fig. 4. The binding pocket of BuChE showing docked conformation of ligand 1-hydroxyanthracene-2,10-dihexanoate (**5**). Conformation shows H-bonds of the ligand with G116, G117 and A199. Red lines represent strong interactions while blue line showing weak interaction. Stability as energy minimization for each bond is represented on the bond representative line. Residues (Green) shown in outline forming other interaction.

Table 3. Energy minimization (in kcal/mol) pattern of docking studies.

Residue	Eserine e.m.[*]	Compound 4 e.m.	Compound 5 e.m.
W82	-2.1	-1	-2.4
G115	–	-10.3	-14.6
G116			
G117			
S198	–	-3.9	-4.1
A199	–	-4.7	-4.7
P285	-4.7	–	–
F329	-0.5	-3.3	-2.8
H438	-2	-6.63	-6.4

[*] e.m. is energy minimization.

W231 and Y332 were failed to interact with compound **5**, in addition to this they seemed not to remain in close proximity.

Enzyme inhibition assay results indicated 1-hydroxyanthracene-2,10-dihexanoate (**5**) to be more potent butyryl cholinesterase inhibitor as compared to standard. Docking studies suggested stable binding of compound **4** and **5** with butyryl cholinesterase at W82, G115, G116, G117, S198, A199, F329 and H438 position forming a strong enzyme inhibitor complex and refraining substrate from binding with active site. Although wet lab experiments indicated compound **5** to be more potent inhibitor as compared to compound **4**, docking studies revealed comparatively stronger interaction between receptor and compound **4** with lower docking energy. The observed high inhibitory activity of compound **5** might be due to the contribution of stereo-chemical stabilizing effects (in dynamic system) on interactions involved in binding and comparatively stable H-bonding with G115, G116, G117, S198 and hydrophobic binding with W82, which in turn stabilizes the hydrophobic interactions with H438 and F329. H438 is a member of the catalytic triad. Although H438 interact with compound **5** with slightly higher energy as compared to compound **4** but might take the advantage of stable H-bonding (Table 3).

4. Conclusion

Newly synthesized anthrarobin acyl derivatives **2–8** were obtained through the reaction of anthrarobin (**1**) and acetic anhydride or acyl chlorides. The compounds **5** and **4** showed remarkable BuChE inhibition potential with IC_{50} values 5.34 and 17.2 µM, respectively when compared with the standard eserine. These bioactive constituents may be considered as the potential candidates for drug development to

treat Alzheimer's disease. It is suggested to perform further *in-vivo* studies to evaluate the toxicity of compounds in animal models.

Declarations

Author contribution statement

Funding statement

Competing interest statement

The authors declare no conflict of interest.

Additional information

Supplementary content related to this article has been published online at http://dx.doi.org/10.1016/j.heliyon.2017.e00350.

References

Aisen, P.S., Davis, K.L., 1997. The search for disease-modifying treatment for Alzheimer's Disease. Neurology 48, S35–S41.

Arnold, S.E., Kumar, A., 1993. Reversible dementias. Med. Clin. North Am. 77, 215–230.

Bachman, D.L., Wolf, P.A., Linn, R.T., 1992. Prevalence of dementia and probable senile dementia of the Alzheimer type in the Framingham study. Neurology 42, 115–119.

Çokuğraş, A.N., 2003. Butyrylcholiesterase: structure and physiological importance. Turk. J. Biochem. 28, 54–61.

Campiani, G., Fattorusso, C., Butini, S., Gaeta, A., Agnusdei, M., Gemma, S., Persico, M., Catalanotti, B., Savini, L., Nacci, V., Novellino, E., Holloway, H.W., Greig, N.H., Belinskaya, T., Fedorko, J.M., Saxena, A., 2005. Development of molecular probes for the identification of extra interaction sites in the mid-gorge and peripheral sites of butyrylcholinesterase BuChE; Rational design of novel, selective, and highly potent BuChE inhibitors. J. Med. Chem. 48, 1919–1929.

Ellman, G.L., Courteny, D.K., Andres Jr., V., Feather-stone, R.M., 1961. A new and rapid colorimetric determination of acetylcholinesterase activity. Biochem. Pharmacol. 7, 88–95.

Giacobini, E., 2001. Selective inhibitors of butyrylcholinesterase: a valid alternative for therapy of Alzheimer's disease? Drugs Aging 18, 891–898.

Greig, N.H., Utsuki, T., Ingram, D.K., Wang, Y., Pepeu, G., Scali, C., Yu, Q.S., Mamczarz, J., Holloway, H.W., Giordano, T., Chen, D., Furukawa, K., Sambamurti, K., Brossi, A., Lahiri, D.K., 2005. Selective butyrylcholinesterase inhibition elevates brain acetylcholine, augments learning and lowers Alzheimer beta-amyloid peptide in rodent. Proc. Natl. Acad. Sci. 102, 17213–17218.

Greig, N.H., Utsuki, T., Yu, Q., Zhu, X., Holloway, H.W., Perry, T., Lee, B., Ingram, D.K., Lahiri, D.K., 2001. A new therapeutic target in Alzheimer's disease treatment: attention to butyrylcholinesterase. Curr. Med. Res. Opin. 17, 159–165.

Hebert, L.E., Scherr, P.A., Beckeff, L.A., Albert, M.S., Pilgrim, D.M., Chown, M.J., Funkenstein, H.H., Evans, D.A., 1995. Age-specific incidence of Alzheimer's disease in a community population. J. Am. Med. Assoc. 273, 1354–1359.

Hiipakka, R.A., Zhang, H.Z., Dai, W., Dai, Q., Liao, S., 2002. Structure-activity relationships for inhibition of human 5α-reductases by polyphenols. Biochem. Pharmacol. 63, 1165–1176.

Kovarik, Z., Bosak, A., Sinko, G., Latas, T., 2003. Exploring the Active Sites of Cholinesterases by Inhibition with Bambuterol and Haloxon. Croatica Chemica Acta 76, 63–67.

Lateef, M., Perwaiz, S., Sidduqui, B.S., Azhar, A., Iqbal, L., Azhar, K.F., Sidduiqui, K., Abbassi, K., 2015. Antioxidant potential of anthrarobin (1, 2, 10-trihydroxyanthracene) and its acyl derivatives. J. Chem. Soc. Pak. 37, 1015–1019.

Macdonald, I.R., Martin, E., Rosenberry, T.L., Darvesh, S., 2012. Probing the peripheral site of human butyrylcholinesterase. Biochem. 51, 7046–7053.

Masson, P., Xie, W., Froment, M.T., Levitsky, V., Fortier, P.L., Albaret, C., Lockridge, O., 1999. Interaction between the peripheral site residues of human butyrylcholinesterase, D70 and Y332, in binding and hydrolysis of substrates. Biochim. Biophys. Acta 1433, 281–293.

Nicolet, Y., Lockridge, O., Masson, P., Fontecilla-Camps, J.C., Nachon, F., 2003. Crystal structure of human butyrylcholinesterase and of its complexes with substrate and products. J. Biol. Chem. 278, 41141–41147.

O'Boyle, N.M., Banck, M., James, C.A., Morley, C., Vandermeersch, T., Hutchison, G.R., 2011. Open Babel: An open chemical toolbox. J. Cheminf. 3, 33.

Perry, E.K., Tomlinson, B.E., Blessed, G., Bergmann, K., Gibson, P.H., Perry, R. H., 1978. Correlation of cholinergic abnormalities with senile plaques and mental test scores in senile dementia. Br. Med. J. 2, 1457–1459.

Quinn, D.M., 1987. Acetylcholinesterase: enzyme structure, reaction dynamics and virtual transition states. Chem. Rev. 87, 955–979.

Rarey, M., Kramer, B., Lengauer, T., Klebe, G., 1996. A fast flexible docking method using an incremental construction algorithm. J. Mol. Biol. 261, 470–489.

Schneider, L.J., 2001. Treatment of Alzheimer's disease with cholinesterase inhibitors. Clin. Geriatr. Med. 17, 337–358.

Sheu, S.Y., Chiang, H.C., 1997. Inhibition of xanthine oxidase by hydroxylated anthraquinones and related compounds. Anticancer Res. 17, 3293–3297.

Woo, Y.J., Lee, B.H., Yeun, G.H., Kim, H.J., Won, M.H., Kim, S.H., Lee, B.L., Park, J.H., 2011. Selective butyrylcholinesterase inhibitors using polyphenol-polyphenol hybrid molecules. Bull. Korean Chem. Soc. 32, 2593–2598.

Wright, C.I., Geula, C., Mesulam, M.M., 1993. Neurological cholinesterases in the normal brain and in Alzheimer's disease: relationship to plaques, tangles, and patterns of selective vulnerability. Annals Neurol. 34, 373–384.